Electrical resistivity, high-resolution thermal expansion, and heat capacity measurements of the charge-density wave compound γ-Mo_4O_{11}

M. S. da Luz, A. de Campos, B. D. White, and J. J. Neumeier
Department of Physics, Montana State University, P.O. Box 173840, Bozeman, Montana 59717-3840, USA
(Received 23 February 2009; revised manuscript received 8 May 2009; published 18 June 2009)

Electrical resistivity of γ-Mo_4O_{11} single crystals was measured using the Montgomery method. The results show a much smaller anisotropy than previously reported. High-resolution linear thermal expansion measurements reveal strongly anisotropic behavior. Both electrical resistivity and thermal expansion measurements suggest that this material should be classified as quasi-two dimensional. The thermal expansion coefficients exhibit an anomaly due to the charge-density wave transition along the *b* and *c* axes at ~100 K.

DOI: 10.1103/PhysRevB.79.233106 PACS number(s): 74.25.Bt, 65.40.De, 65.40.Ba

Low-dimensional materials have attracted a great deal of theoretical and experimental attention during the last two decades because of their unusual chemical and physical properties. One particularly salient property common to many low-dimensional systems is a charge-density wave (CDW), which has been intensively studied after the suggestion by Peierls that a metallic chain would be unstable in one dimension.[1] It is well known that the CDW instability strongly depends on the dimensionality of the electron system and is often observed in quasi-one-dimensional (quasi-1D) or two-dimensional (2D) conductors, where a good nesting condition between two parallel Fermi surfaces is more easily fulfilled.[2] The transition to a CDW state is a genuine thermodynamic phase transition driven by strong electron-phonon coupling and can have a dramatic affect on physical properties.[3]

Tungsten and molybdenum oxides such as η- and γ-Mo_4O_{11} have been studied extensively as model CDW materials.[4–8] Both η- and γ-Mo_4O_{11} exhibit 2D metallic electrical resistivity at room temperature. The γ phase, which is stabilized at high temperature and retained by quenching to room temperature[5,9] (the transition temperature from γ to η is ~610 °C), has orthorhombic symmetry ($Pn2_1a$) with lattice parameters[10] a=24.487 Å, b=5.457 Å, and c =6.752 Å. It consists of infinite slabs of distorted MoO_6 octahedra, parallel to the *b*-*c* plane, connected by MoO_4 tetrahedra (see Fig. 1). The conduction electrons are confined in the octahedral slabs, which leads to a partially filled conduction band in the *b*-*c* plane and a quasi-2D electronic structure.[10] The difference between the η and γ phases lies in the arrangement of successive MoO_6 slabs; the adjacent slabs have the same orientation in η-Mo_4O_{11} but are mirror images with respect to the *b*-*c* plane in γ-Mo_4O_{11}. The γ phase has an incommensurate CDW transition at ~100 K with its structural modulation along *b*. Electrical transport properties suggest that γ-Mo_4O_{11} is a quasi-2D metal below 100 K.[4,11,12]

In all measurements of γ-Mo_4O_{11} up to now, electrical resistivity was determined using a standard four-probe technique[4,12] where the current is applied along the same direction that the voltage is measured; the ratio of voltage to current is then used to calculate the resistance along that crystallographic axis. However, in low-dimensional materials it is well known[13] that this simple method yields sizable errors because of current leakage along the other two axes. The well-known Montgomery[13] method is the accepted manner of adjusting for this and ultimately determining the correct values of the electrical resistivity along each axis; these values correspond to the diagonal components of the electrical resistivity tensor.

In this work, the anisotropic electrical resistivity along the principal crystallographic directions of γ-Mo_4O_{11} was measured and the diagonal components of the electrical resistivity tensor were determined using the Montgomery method.[13] The results confirm the quasi-2D nature but reveal a smaller anisotropic-resistivity ratio than previously reported.[4,12] Our high-resolution thermal expansion measurements exhibit strong anisotropy between the *b*-*c* plane and *a* axis but also support designation of γ-Mo_4O_{11} as quasi-2D. The thermal expansion coefficients show anomalies due to the CDW transition at ~100 K that are more subtle than what is observed in some other CDW systems.[3] Heat capacity was measured but no feature is evident near 100 K within our resolution.

Single crystals of γ-Mo_4O_{11} were grown using a temperature-gradient flux method.[14] The samples used in this

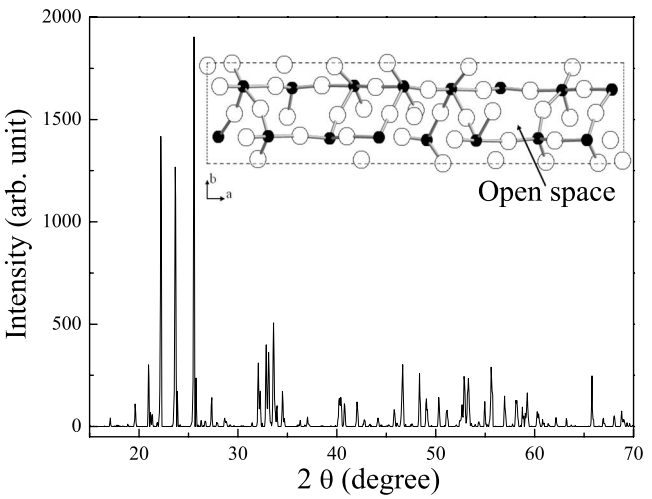

FIG. 1. X-ray powder-diffraction data for γ-Mo_4O_{11}. All Bragg reflections correspond to those of the γ-Mo_4O_{11} structure as reported by Ghedira *et al.* (Ref. 10). Inset shows the crystal structure projected onto the (001) plane, where the solid circles represent Mo ions and open circles oxygen ions.

 ©2009 The American Physical Society

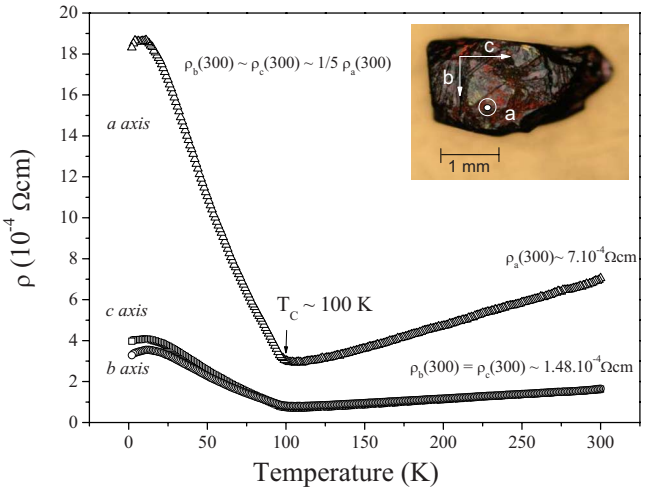

FIG. 2. (Color online) Electrical resistivity versus temperature for the three principal crystallographic directions of γ-Mo_4O_{11}. The resistivity values at 300 K for each axis are indicated. A photograph of a representative crystal and its orientation is shown in the inset.

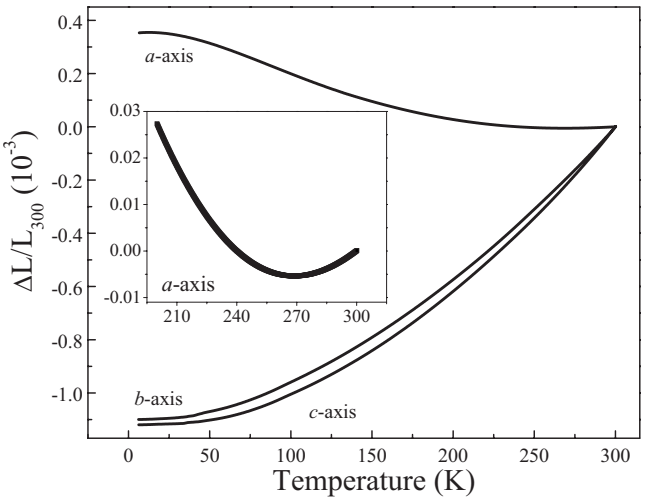

FIG. 3. Linear thermal expansion ($\Delta L/L_{300}$) for the three principal crystallographic directions. The inset shows the beginning of the negative thermal expansion near 270 K in the a axis.

work had typical dimensions of $\sim 2.0 \times 1.5 \times 0.5$ mm^3 with the large face corresponding to the b-c (100) crystallographic plane (see inset, Fig. 2). Two crystals were oriented using back-reflection Laue x-ray diffraction and carefully polished to obtain rectangular shapes for better determination of the geometric factors. The polished crystals had sizes $0.11 \times 0.827 \times 0.605$ and $0.184 \times 0.525 \times 0.631$ mm^3 (a, b, and c axes, respectively). Low-resistance gold contacts were deposited on the samples for measuring the four-probe electrical resistance and the Montgomery method[13] was used to determine the electrical resistivity. We report the average of three measurements in each direction and the corresponding uncertainties. Thermal expansion was measured on the same crystals using a capacitive dilatometer cell constructed from fuzed quartz.[15] It can detect 0.1 Å changes in specimen length for a relative resolution of about 10^{-8}; this resolution is about 4 orders of magnitude higher than that possible with diffraction techniques. Data are collected at an interval of 0.2 K while warming at 0.20(1) K/min. The data are corrected for the thermal expansion of fused quartz.[15] Heat capacity at constant pressure, C_P, was measured using a Quantum Design physical property measurements system (PPMS).

Figure 1 displays the x-ray powder-diffraction pattern of γ-Mo_4O_{11} crystals that were ground into a powder for the measurements. All Bragg reflections were indexed to an orthorhombic unit cell with space group $Pn2_1a$ in excellent agreement with reported structural refinements of γ-Mo_4O_{11} simulated by POWDERCELL.[10,16] The inset shows the crystal structure of the γ phase. The structural framework of γ-Mo_4O_{11} contains two uniquely coordinated polyhedra: regular MoO_4 tetrahedra and distorted MoO_6 octahedra. All octahedra share their corner oxygen ions to form stacked quasi-2D layers which are connected by the tetrahedra. Also, two open spaces can be found within the orthorhombic structure.

Figure 2 shows the electrical resistivity ρ versus temperature determined using the Montgomery procedure.[13] The anisotropy in $\rho(T)$ suggests that γ-Mo_4O_{11} can be thought of as a 2D metal since $\rho_b \sim \rho_c$ and ρ_a is greater than ρ_b and ρ_c. In the b-c plane, $\rho(T)$ exhibits a phase transition at $T_C \sim 100$ K with weak temperature dependence above this temperature. Below T_C, the resistivity increases monotonically with decreasing temperature, with the strongest temperature dependence along a. This transition is due to a charge-density wave[4,12] that is associated with the quasi-2D electronic properties. The Fermi surface is expected to be strongly anisotropic and to show large regions parallel to the a axis leading to nesting properties.[4] In related 2D conductors with a CDW transition, such as the potassium purple bronze KMo_6O_{17}, the resistivity decreases again with the temperature well below T_C.[4] In η-Mo_4O_{11}, $\rho(T)$ exhibits a second transition[17] near $T \sim 30$ K corresponding to a second instability in the Fermi surface. In our γ-Mo_4O_{11} samples, the decrease in $\rho(T)$ near 10 K might be interpreted as a signature of a second transition but the thermal expansion and C_P measurements (see below) do not support this. Furthermore, the CDW gaps in γ-Mo_4O_{11} continue[9] to open down to 4.2 K.

Returning to the anisotropy of γ-Mo_4O_{11}, the average resistivities at 300 K based on the results of three different measurements for two single crystals are $\rho_a = 7.1(4) \times 10^{-4}$ Ω cm and $\rho_b \simeq \rho_c \simeq 1.48(8) \times 10^{-4}$ Ω cm. Using the resistivities at 300 K, one can estimate the anisotropic resistivity ratio as $\rho_b \simeq \rho_c \simeq \frac{1}{5}\rho_a$, which differs significantly from the reports of Schlenker and Sato, Nakao and Hoshino of $\rho_b \simeq \rho_c \sim \frac{1}{100}\rho_a$.[4,12] This difference is associated with our use of the Montgomery method.[13]

Linear thermal expansion (LTE), normalized to the length at 300 K($\Delta L/L_{300}$) along the three principal crystallographic directions, is displayed in Fig. 3. The results reveal strongly anisotropic behavior. The in-plane LTEs (b and c axes) are about three times larger in magnitude than that of the a axis. The LTE has the same behavior for the b and c axes with little difference in magnitude between them. Along the a axis, the crystal contracts from room temperature to ~270 K followed by an expansion with further cooling (see inset of

Fig. 3). The observed anisotropy in $\Delta L/L_{300}$ further confirms the characterization from $\rho(T)$ measurements of this material as quasi-2D. This is a clear distinction from quasi-1D materials such as $Li_{0.9}Mo_6O_{17}$, where both $\Delta L/L_{300}$ and ρ have 1D character.[18,19]

Negative thermal expansion (NTE) of materials over an extended temperature range is an unusual structural property with a variety of potential technological applications. Only a few families of cubic materials (isotropic materials) are known to exhibit considerable NTE behavior such as AM_2O_8 (A=Zr or Hf; M=V), AM_2O_7 (A=U, Th, Zr, Hf or Sn; M=P,V), cuprite structures (Cu_2O and Ag_2O), some tetrahedrally coordinated structures (CuCl), and some zeolites/zeolitelike materials.[20] However, even when the volumetric thermal expansion coefficient is positive, one or two of the three principal linear coefficients may be negative. That is the case in γ-Mo_4O_{11} and in other anisotropic materials such as $Li_{0.9}Mo_6O_{17}$.[18] Another example is η-Mo_4O_{11}, which exhibits almost isotropic thermal expansion above T_C, while below T_C the lattice parameters determined by x-ray diffraction reveal strong NTE along the a axis and possible NTE along b.[21] Various mechanisms have been proposed to explain the NTE in anisotropic materials.[20] Generally, NTE along a single crystallographic axis can be attributed to the existence of some anomalous phonon modes that result from the low-crystal symmetry.[22]

There are no obvious features in $\Delta L/L_{300}$ near $T_C \sim 100$ K (see Fig. 3) in our data. In η-Mo_4O_{11}, the observed NTE in the CDW state along the a axis sets in Ref. 21 above T_C, and may be associated with the CDW. In the blue bronze $K_{0.3}MoO_3$, a distinct feature appears in the temperature derivative of $\Delta L/L_{300}$, the thermal expansion coefficient[3,23] however, the x-ray data for η-Mo_4O_{11} have insufficient resolution to search for a feature in the thermal expansion coefficient.

Figure 4 displays the linear thermal expansion coefficients, $\mu_i = d(\Delta L/L_{300})/dT$ for the $i=a$, b, and c axes. We determined μ_i by fitting the data in Fig. 3 using Chebyshev polynomials and differentiating, as reported previously.[15] This process includes cross checking with the point-by-point derivative to ascertain that no subtle features are overlooked.[24] Examination of μ_i reveals clear features along b and c and a change in slope along the a axis at $\sim$100 K. These features are associated with the occurrence of the CDW transition. Similar to[8,9] η-Mo_4O_{11}, in γ-Mo_4O_{11} the CDW forms along the b direction and NTE is observed below T_C along a. No feature in the linear thermal expansion coefficients is evident near 10 K, where electrical resistivity measurements reveal a downturn (see Fig. 2). The phase transition at T_C is also clearly evident in the volumetric thermal expansion coefficient $\Omega = \mu_a + \mu_b + \mu_c$, which is dominated by μ_b and μ_c (see Fig. 5). The features along b, c, and Ω are similar in character to those generally associated with a second-order (continuous) phase transition, which ideally are steplike features,[25] as indicated by the dashed lines in the upper insets of Figs. 4 and 5. The observed broadening is probably associated with phase fluctuations. The steplike features at T_C are about 60 times smaller than those observed in the blue bronze.[3] This underscores the value of measuring thermal expansion at high resolution.

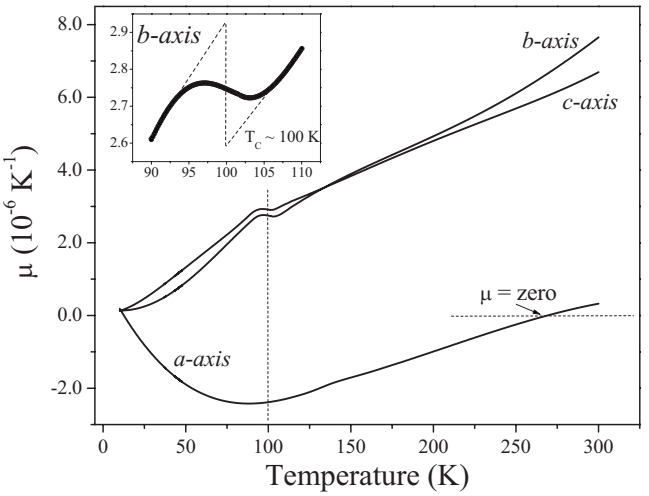

FIG. 4. Thermal expansion coefficient $\mu = (1/L_{300\ K})d\Delta L/dT$ for the three principal crystallographic directions. In the inset, the jump at T_c for the b axis is shown. The vertical dashed line shows the transition temperature at $\sim$100 K and the horizontal dashed line shows the crossover between negative and positive LTE at $\sim$270 K.

The a lattice parameter (similar to $\Delta L/L_{300}$) of η-Mo_4O_{11} exhibits negative thermal expansion below T_C, with the onset slightly above T_C. In contrast, the behavior of $\Delta L/L_{300}$ in γ-Mo_4O_{11} shows little change in behavior in the vicinity of T_C. Perhaps, this is associated with its softer lattice[8,9,11] of η-Mo_4O_{11} when compared to γ-Mo_4O_{11}. A softer lattice may lead to larger features at the CDW transition and maybe the occurrence of two CDW transitions in η-Mo_4O_{11}, as opposed to[4] a single transition in γ-Mo_4O_{11}.

On general thermodynamic grounds, the heat capacity C_P and ΩT should scale with one another in the vicinity of a continuous phase transition (after subtraction of a linear term from ΩT),[25] but in γ-Mo_4O_{11} the CDW transition at $\sim$100 K could not be detected in our C_P measurements

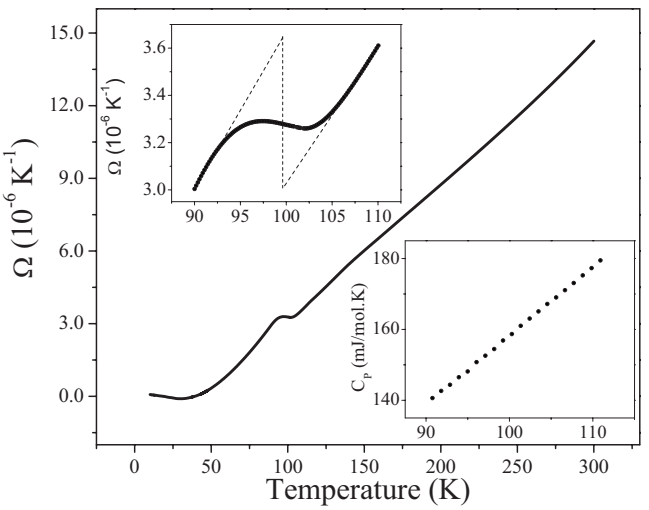

FIG. 5. Volumetric thermal expansion coefficient (Ω) versus T (main panel and upper inset). The lower inset shows heat capacity C_P versus T.

(lower inset, Fig. 5). Other studies failed, as well, to observe a feature[9,11] in C_P. We extracted the Debye temperature (Θ_D), which was found to be ~400 K. This is higher than that reported for the η-phase (Θ_D=330 K),[4] consistent with a stiffer lattice in γ-Mo_4O_{11}. The Debye temperature was obtained using the low-temperature heat capacity and the slope of C_P/T versus T^2 equal to $\beta = (1943.9\ \text{J mol}^{-1}\ \text{K}^{-1})/\Theta_D^3$.

In summary, the electrical resistivity has been determined using the Montgomery method for γ-Mo_4O_{11}. The results confirm the quasi-2D nature but clearly show a much smaller anisotropy than previously reported. LTE reveals anisotropic behavior between the *b*-*c* plane and the *a* axis as well as quasi-2D behavior. Along the *a* axis, the crystal contracts from room temperature to ~270 K followed by an expansion with further cooling. The thermal expansion coefficients exhibit clear features at the CDW transition.

This material is based upon work supported by the Office of Basic Energy Sciences of the Department of Energy under Contract No. DE-FG-06ER46269 and the National Science Foundation under Contract No. DMR-0504769. A.d.C. acknowledges support from CNPq under Contract No. 301334/2007-2. Discussions with C. A. M. dos Santos are greatly appreciated.

[1] R. E. Peierls, *Quantum Theory of Solids* (Oxford University Press, New York, 1955).
[2] G. Grüner, *Density Waves in Solids* (Addison-Wesley, Reading, MA, 1944).
[3] J. W. Brill, M. Chung, Y.-K. Kuo, X. Zhan, E. Figueroa, and G. Mozurkewich, Phys. Rev. Lett. **74**, 1182 (1995).
[4] *Low-Dimensional Electronic Properties of Molybdenum Bronzes and Oxides*, edited by C. Schlenker (Kluwer, Dordrecht, 1989).
[5] *Oxide Bronzes*, edited by M. Greenblatt [special issue of Int. J. Mod. Phys. B **7**, Nos. 23–24 (1993)].
[6] E. Canadell, Chem. Mater. **10**, 2770 (1998).
[7] E. Canadell and M.-H. Whangbo, Int. J. Mod. Phys. B **7**, 4005 (1993).
[8] Z. Zhu, S. Chowdhary, V. C. Long, J. L. Musfeldt, H.-J. Koo, M.-H. Whangbo, X. Wei, H. Negishi, M. Inoue, J. Sarrao, and Z. Fisk, Phys. Rev. B **61**, 10057 (2000).
[9] M. Greenblatt, Chem. Rev. (Washington, D.C.) **88**, 31 (1988).
[10] M. Ghedira, H. Vincent, M. Marezio, J. Marcus, and G. Furcaudot, J. Solid State Chem. **56**, 66 (1985).
[11] H. Guyot, C. Schlenker, G. Fourcaudot, and K. Konaté, Solid State Commun. **54**, 909 (1985).
[12] M. Sato, K. Nakao, and S. Hoshino, J. Phys. C **17**, L817 (1984).
[13] H. C. Montgomery, J. Appl. Phys. **42**, 2971 (1971).
[14] W. H. McCarroll and M. Greenblatt, J. Solid State Chem. **54**, 282 (1984).
[15] J. J. Neumeier, R. K. Bollinger, G. E. Timmins, C. R. Lane, R. D. Krogstad, and J. Macaluso, Rev. Sci. Instrum. **79**, 033903 (2008).
[16] W. Kraus and G. Nolze, J. Appl. Crystallogr. **29**, 301 (1996).
[17] M. Koyano, A. Miyata, and H. Hara, Physica B **284-288**, 1663 (2000).
[18] C. A. M. dos Santos, B. D. White, Yu. Yi-Kuo, J. J. Neumeier, and J. A. Souza, Phys. Rev. Lett. **98**, 266405 (2007).
[19] M. S. da Luz, C. A. M. dos Santos, J. Moreno, B. D. White, and J. J. Neumeier, Phys. Rev. B **76**, 233105 (2007).
[20] G. D. Barrera, J. A. O. Bruno, T. H. K. Barron, and N. L. Allan, J. Phys.: Condens. Matter **17**, R217 (2005).
[21] H. Negishi, Y. Kuroiwa, H. Akamine, S. Aoyagi, A. Sawada, T. Shobu, S. Negishi, and M. Sasaki, Solid State Commun. **125**, 45 (2003).
[22] N. A. Abdullaev, Phys. Solid State **43**, 727 (2001).
[23] M. L. Tian, L. Chen, and Y. H. Zhang, Phys. Rev. B **62**, 1504 (2000).
[24] The capacitance channel has a resolution of one part in 10^8 while the temperature channel has a resolution of one part in 10^5. This and the close spacing between data points leads to scatter in the temperature derivative of $\Delta L/L_{300}$, that is, most noticeable in smooth regions of the measurement range. Our fitting procedure minimizes this scatter.
[25] J. A. Souza, Y.-K. Yu, J. J. Neumeier, H. Terashita, and R. F. Jardim, Phys. Rev. Lett. **94**, 207209 (2005).